Exploration of the Conformational Space of a Polymeric Material that Inhibits Human Immunodeficiency Virus

Tulay Ercanli and Donald B. Boyd*

Department of Chemistry and Chemical Biology, Indiana University−Purdue University at Indianapolis, 402 North Blackford Street, Indianapolis, Indiana 46202-3274

Received August 22, 2005

Baertschi et al. (*Antiviral Chem. Chemother.* **1997**, *8*, 353−362) clarified the nature of a polymeric degradation product formed from the cephalosporin ceftazidime. Interest in the polymeric material arises from its ability to inhibit the RNase H and polymerase activities of HIV-1 reverse transcriptase (RT). To shed light on the structure of the polymeric material like that which forms from degradation of third-generation cephalosporins, we apply molecular modeling and other computational chemistry techniques. Aminothiazole methoxime (2-amino-4-thiazolyl-methoxyimino; ATMO) is the parent structure related to the isolated degradation product of ceftazidime. The MMFF94 force field and Monte Carlo multiple minimum method as implemented in MacroModel are used to generate low-energy conformers. We built up oligomeric models starting from the trimer to the 16-mer and performed distribution analyses on the dihedral angles from the Monte Carlo runs to analyze the three-dimensional shapes of the oligomers. Although the larger oligomers are too long for a complete search of conformational space, the low-energy conformers examined do not show secondary structure or repetitive conformations. Polymeric ATMO material may, therefore, exhibit only random coil conformations. Topological similarity of ATMO structures to other reported RT inhibitors is also examined.

INTRODUCTION

Reverse transcriptase of human immunodeficiency virus (HIV-1 RT) synthesizes double-stranded DNA from proviral RNA. There are many marketed drugs and investigational compounds that target the RNA-dependent DNA polymerase activity of RT.[1−4] However, there is no drug yet marketed to inhibit specifically the RNase H activity of RT, although the attractiveness of their target has been discussed in the literature.[5−10] RNase H degrades the RNA strand of the RNA/DNA hybrid during reverse transcription.[11]

HIV-1 RT sustains transcription error rates as high as 3.4×10^{-5} per base pair per replication cycle, thus allowing drug-resistant variants with different genetic codes for RT to evolve rapidly. The present therapy for coping with this troublesome issue is to inhibit simultaneously more than one step in virus replication by administering combinations of drugs with different enzyme targets.[7] In other words, resistant virus mutants are less likely to develop when cocktails of available agents are used to treat patients. Highly active antiretroviral therapy staves off death but does not cure the disease. Hence, more effective treatments for AIDS constitute an unmet medical need.

HIV-1 reverse transcriptase consists of two chains, which are folded in the well-known hand shape.[12−14] RNase H is a subdomain of HIV-1 RT on chain A (p66). The polymerase-dependent activities of RNase H cleave RNA from the RNA/DNA duplex occurring with DNA polymerization. On the other hand, polymerase-independent activities of RNase H involve hydrolysis in the absence of polymerization.[8] RNase H-mediated events are very important for HIV-1 replication, and without this activity, double-stranded viral DNA cannot be achieved. Two studies of RT-RNase H inhibitors are summarized as follows.

Min et al., working on natural sources of drugs, observed that the extract of *Juglans mandshurica* (stem-bark) had activity (IC_{50} of 22 μg/mL) against RNase H function and an IC_{50} of 0.047 μg/mL against RT activity.[5] They also investigated RNase H activity inhibition by quinones and demonstrated that some naphthoquinones had significant potential. A nonhydroxylated naphthoquinone had an IC_{50} of 9.5 μM.[6]

Shaw-Reid and co-workers found that a diketo acid, 4-[5-(benzoylamino)thien-2-yl]-2,4-dioxobutanoic acid, selectively inhibits the RNase domain of RT. The enzymatic activity requires Mn^{2+}, so this metal-dependent mechanism is similar to the inhibition mechanism of integrase inhibitors of the same structural class. Therefore, potent integrase inhibitors can be tested for RNase H activity also.[10]

Intriguing to us is a little-studied cephalosporin-derived material that inhibits HIV-1 RT. Cephalosporins are well-known β-lactam compounds with the ability to cure infections caused by Gram positive and Gram negative bacteria. Scientists were not aware of much antiviral activity of these compounds until 1987 when Swiss scientists made the curious observation that eukaryotic DNA polymerase α was inhibited by antibiotics.[15] Cephalosporins were 20 times more active than penicillins, whereas monobactam antibacterials were ineffective. The Swiss group also found that DNA polymerases and HIV-1 reverse transcriptase have some sequence homologies to penicillin binding proteins, which are also the targets of cephalosporins.[16] In 1991, Hafkemeyer et al. purified and determined the structure of a degradation product (HP 0.35) formed from the 7-position side chain of

* To whom correspondence should be addressed. E-mail: boyd@chem.iupui.edu; tel.: 317-274-6891; fax: 317-274-4701.

10.1021/ci050339a CCC: $33.50
Published on Web 01/05/2006

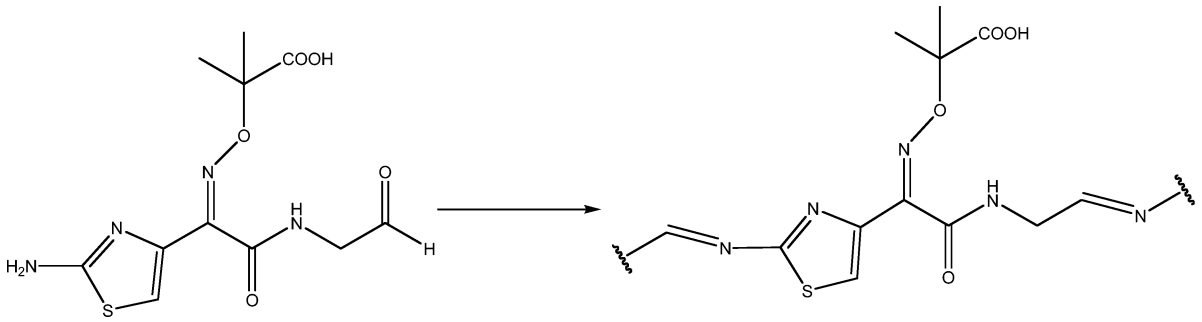

Figure 1. Reaction of the monomer aldehyde forming a polymer by amino−aldehyde condensation to the imine.

the cephalosporin ceftazidime. The purified aldehyde HP 0.35 was claimed to have an inhibitory effect on the RNase H activity of HIV-1 reverse transcriptase.[17]

In 1997, Baertschi et al.[18] demonstrated that inhibitory activity of the isolated fractions of the ceftazidime degradation products is not directly related to the relative amount of purified aldehyde (HP 0.35) present. In fact, the IC_{50} values of HP 0.35 against the HIV-1 RT polymerase and RNase H activities were > 100 μg mL^{-1}. The Lilly group further showed that, when the aldehyde degradation product from ceftazidime polymerizes (Figure 1), the potency against the polymerase and the RNase H activities in vitro improved (IC_{50} values of approximately 0.1 and 0.01 μg mL^{-1}, respectively). Thus, ceftazidime high molecular weight polymer (HMWP) had a high inhibitory effect on the polymerase and especially on the RNase H activities of HIV-1 RT. As the polymerization in a sample of aldehyde from ceftazidime degradation increased (up to about 10 kDa), the antiviral activity also increased. No evidence indicated that HMWP's bioactivity arose solely from its polyanionic nature. Baertschi et al. concluded that HMWP is an interesting inhibitor of HIV-1 RT RNase H and polymerase activities deserving further study. However, the mechanism of action and the chemical nature of this polymer were not further explored because of changing corporate priorities.

A 2001 response by the Swiss group[19] confirmed that the polymer is a high molecular weight fraction (MW 8000) from hydrolyzed ceftazidime, and it inhibited both HIV-1 RT polymerase and RNase H. The mild degradation conditions indicate that it is a homopolymer. Hobi et al. speculated that HMWP may also block an earlier step in viral replication, but a promised follow-up study has not yet been published. Beyond this handful of papers, little has been reported about the antiviral polymeric material.

Independently, it was found that HIV-1 RT inhibition is not limited to degradation products of ceftazidime.[20] A number of third-generation cephalosporins that had an opportunity to degrade during normal storage conditions exhibit anti-HIV activity. Cephalosporin powders and crystals in a bottle or other storage container become more acidic as they age. Baertschi et al. showed that acidic (as well as basic) conditions catalyze polymerization of the degradation products.[18] Significantly, the carboxylic group of the oxyimino side chain of ceftazidime is not a structural requirement for anti-HIV activity. Hence, we believe that many third-generation cephalosporins, that is, those with an aminothiazole methoxime (2-amino-4-thiazolyl-methoxyimino; ATMO) in the 7-acylamido side chain, are capable of forming polymeric material that inhibits HIV. The general formula is

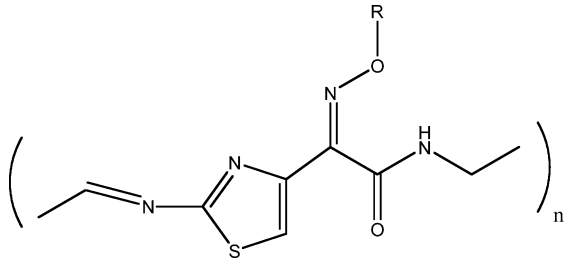

where R is a methyl, 1-carboxy-1-methylethyl, or other group.

Physical, chemical, and biological properties of enzyme inhibitors depend on their chemical structure and conformations. This paper is the first one that focuses on molecular modeling and conformational flexibility of a polymeric material like that which forms from degradation of third-generation cephalosporins. A priori, we had no reason to expect an ATMO-containing polymer to prefer a specific secondary structure. The ATMO polymer does not have the same sites for intramolecular hydrogen bonding as do polymers of nucleic acids and amino acids. Hence, we began the modeling with no preconceived ideas on what the ATMO polymer should look like.

Since the ceftazidime degradation product has a molecular weight of 8000, it is roughly a 40-mer. Modeling such a large structure is beyond the scope of this work. First, we want to gain a better understanding of smaller oligomers formed from the ATMO subunits. Even for these, a complete search for conformational space is impractical. Hence, we employed Monte Carlo (MC) simulations to explore conformational possibilities. We built model oligomers starting from the trimer up through the 16-mer and analyzed their conformational preferences. We used the information generated from each small oligomer to build the next size larger.

In addition to the model building, we quantified the molecular similarity between the ATMO and other recently reported HIV RNase H and RT inhibitors.

METHODOLOGY

The MMFF94 and MMFF94s force fields were validated to be the best overall computational chemistry methods at reproducing crystallographic data and conformational properties of the ATMO moiety.[21] The two force fields performed about equally well. We selected the MMFF94 force field as

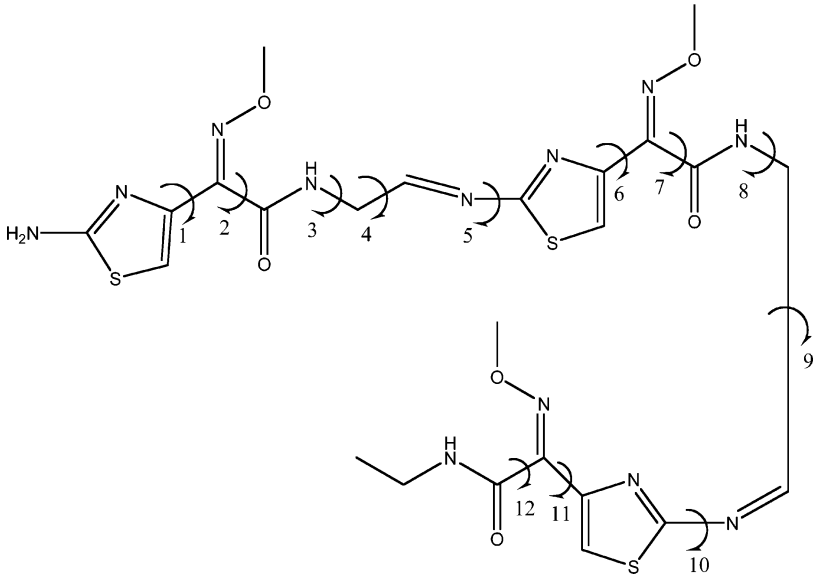

Figure 2. Numbering system for rotatable bonds in the trimer. Dihedral angle 1 is defined as $N-C_{sp^2}-C_{sp^2}=N$, 2 as $C_{sp^2}-C_{sp^2}-C_{sp^2}-N$, 3 as $C_{sp^2}-N-C-C_{sp^2}$, 4 as $N-C-C_{sp^2}=N$, and 5 as $C_{sp^2}=N-C_{sp^2}=N$. To simplify the model, the amide and imine bonds, which can isomerize under some conditions, were assumed in this initial work to be nonrotatable, likewise for the N-ethyl end group.

implemented in the molecular modeling program MacroModel (version 8.6) in Maestro[22] (version 6.5) to model the ATMO oligomers. We employed the Monte Carlo multiple minimum (MCMM)[23,24] method in MacroModel to generate sets of low-energy conformers of each oligomer. The calculations were run on two Silicon Graphics Octane workstations (dual R12000 processors operating under IRIX64 6.5.20m with 1.28 GB of memory).

Other molecular modeling programs including SYBYL, Spartan, Cerius2, and InsightII/Discover were also examined but were not as useful for meeting our needs of (1) running conformational searches of organic molecules with up to 400 atoms and many rotatable bonds, (2) using the MMFF94 force field, (3) selecting some torsional angles to be free to rotate but constraining others, and (4) analyzing the results from the conformational searches and being able to export the results to other programs for further analysis.

For each oligomer, we first energy-minimized the structure and then set up the MCMM run. MCMM performs a random walk through conformational space. Random changes are made in torsional angles during the search. We used the default minimum and maximum rotations 0° and ±180° for each rotatable bond. There is no limit on the number of torsions set for rotation, although it is preferable but not always practical to have at most 10−15 torsions free to rotate in each MCMM run. The number of steps is set depending on the computer time available and how many steps are needed to get a fair sampling of conformers.

The MacroModel algorithm[28,29] involves random generation of new conformations and then checking if the energy of these is within an energy window of 25 kJ/mol; we did not energy-minimize the conformers during this process. The algorithm compares each newly generated structure with low-energy conformers that were already found during the MCMM search. MacroModel does this comparison by rigid superimposition of heavy atoms (nonhydrogenic atoms). If the structure is judged not to be a duplicate of a previous structure, it is saved. Then, a new search cycle is started by using the most recent structure as the initial geometry. The simulations on the oligomers generally ran 1−3 days each.

After each MC run, we optimized the lowest-energy conformer encountered. For this minimization, implicit solvation[25,26] was invoked to mimic the effect of water on the oligomer.

We initially did multiple exploratory runs of the ATMO trimer. We proceeded to do calculations on the tetramer, pentamer, and hexamer. Subsequently, we increased the oligomer length in steps of two and thereby treated the octamer, decamer, 12-mer, 14-mer, and finally the 16-mer. Thus, we examined larger and larger oligomers in a build-up procedure. Our build-up method is somewhat reminiscent of Scheraga's method for polypeptides.[27,28] We sometimes used the lowest-energy conformer found for one size oligomer to construct the next larger oligomer. However, we also started some of the MC runs from extended conformers.

We investigated using the preferred dihedral angles found for the smaller oligomers to set up the MC runs for larger oligomers. Hence, we exported the output data from Maestro to the interactive graphical statistics program JMP[29] running on a PC. JMP was used to perform a distribution analysis on the dihedral angles of the ensemble of low-energy conformers generated in each MC simulation. The resulting histograms reveal how frequently specific torsional angle values occur in the structures. The XCluster program in Maestro was also used to generate families of conformers depending on geometrical similarity, but the output of XCluster was much less useful.

Finally, to compare quantitatively the similarity between the chemical diagrams of ATMO and other HIV-1 inhibitors, we calculated Daylight fingerprint similarity[30,31] expressed as Tanimoto coefficients. We employed a program on the Internet.[32,33] A fingerprint is a fixed-length, binary bit vector describing the presence or absence of structural features. The fingerprinting algorithm looks for structural features such as an atom or sets of atoms and bonds connected by two up through seven bond paths long. The molecular similarity program requires structures in SMILES notation.[34] Hence, chemical diagrams were drawn into ChemDraw[35,36] to generate SMILES, and then, the SMILES were pasted into

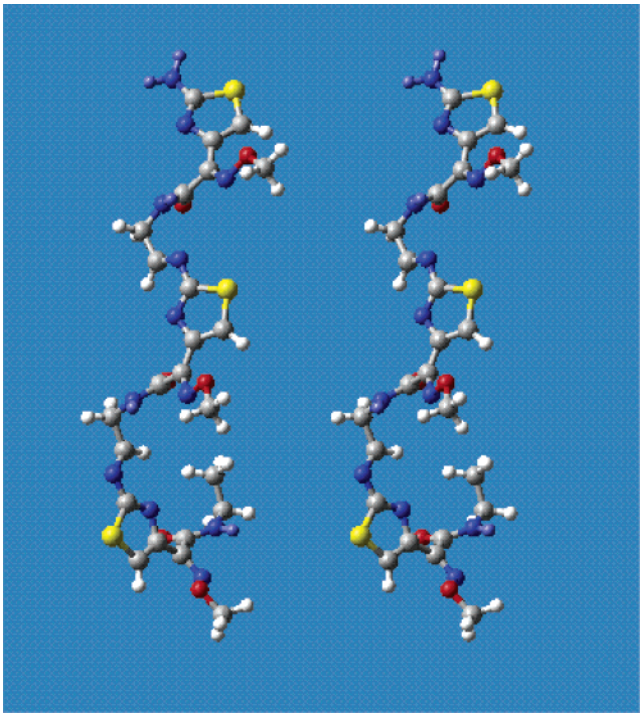

Figure 3. Stereoview of the lowest-energy trimer conformer resulting from the MC conformational search.

the website program. The Tanimoto coefficient is defined as the ratio $c/(a + b - c)$, where a is the number of bits in the fingerprint representation of structure 1, b is the number of bits in structure 2, and c is the number of bits which are common to both structures. Hence, the Tanimoto coefficient ranges from 0.0 (no similarity whatsoever) to 1.0 (perfect match).[37]

RESULTS AND DISCUSSION

Oligomer Modeling. We built the initial structure of the trimer by appropriately linking three monomer units of the ATMO model from our previous work.[21] The amide was placed in a trans configuration and the oxime in an E configuration.[38] In future work, we would like to examine other configurational possibilities for the polymer model. Variable torsional angles for the trimer structure are shown in Figure 2.

After minimizing the trimer with the MMFF94 force field in MacroModel/Maestro, we set up the MCMM simulation as follows. The number of steps was set to 500 000, and 12 rotatable bonds were marked for conformational exploration. The MC run stopped at 341 133 steps as a result of running out of computer memory. This number of steps was sufficient for generating 8105 allowed conformers. These allowed conformers are the ones that had energies within MacroModel's energy window of 25 kJ/mol and that did not duplicate any of the stored conformers. The lowest-energy conformer (Figure 3) had a molecular mechanics energy of 719.407 kJ/mol. When this structure was minimized with implicit water as the solvent, the energy dropped to 581.509 kJ/mol and the structure remained closely similar to the one depicted in Figure 3. We summarize the results for the trimer and the remaining oligomers in Table 1. We exported the output data from Maestro into JMP for a distribution analysis. This revealed that most of the conformers (see Figure 2) had dihedral angle 2 near −142°, dihedral angle 3 near 96°, dihedral angle 6 near −141°, dihedral angle 8 near 87°, and dihedral angle 10 near 2°. The remaining dihedral angles were widely distributed or clustered in multiple small peaks.

The tetramer was built by adding a monomer to the energy-minimized trimer structure and then minimizing this initial geometry. We tried to make the conformational search more efficient by assuming that torsions found to exist in a very narrow range in the trimer could be constrained in the tetramer, thereby decreasing the number of freely rotatable bonds that would be explored in the MC runs. Hence, we put constraints on five torsions to hold them near the trimer values reported in the above paragraph. Twelve rotatable bonds were marked for exploration. The lowest-energy conformer is shown in Figure 4, and minimization did not change the shape of the structure appreciably for the tetramer or any of the larger oligomers discussed in this paper. Distribution analysis results indicated that certain torsional angles were narrowly distributed: dihedral angle 11 values peaked near 144°, dihedral angle 12 near 43°, dihedral angle 13 near 132°, dihedral angle 14 near −65°, dihedral angle 15 near −31°, dihedral angle 16 near 138°, and dihedral angle 17 near 90° (Figure 5). The remaining torsions (rotatable bonds 1, 4, 5, 7, and 9) were widely distributed. Other numerical results are summarized in Table 1.

We built the pentamer by adding a monomer to the energy-minimized tetramer just discussed. When preparing the MC conformational search, we put constraints on 13 dihedral angles found to be roughly invariant in the tetramer distribution analysis. We used the torsional angles as reported in the paragraphs above on the trimer and tetramer. Nine rotatable bonds were designated for exploration. Distribution analysis results from JMP showed no highly preferred values for the free dihedral angles. The shape of the lowest-energy

Table 1. Results of Monte Carlo Multiple Minimum Simulations

oligomer	number of Monte Carlo steps	number of allowed conformations found	energy of lowest allowed conformation (kJ/mol)	energy of lowest energy conformer after minimization (kJ/mol)
trimer	371 133	8105	719.407	581.509
tetramer	300 000	3231	1011.017	850.684
pentamer	300 000	8514	1323.474	1116.570
hexamer	300 000	2851	1613.808	1381.796
octamer	300 000	3438	2474.879	1919.864
decamer	800 000	1659	2868.536	2403.486
12-mer	600 000	2037	3633.100	2945.616
14-mer	600 000	1868	4152.111	3473.582
16-mer	600 000	349	4735.815	4009.209
16-mer	650 000	454	4795.262	4008.966
16-mer	600 000	1111	4708.950	4012.170

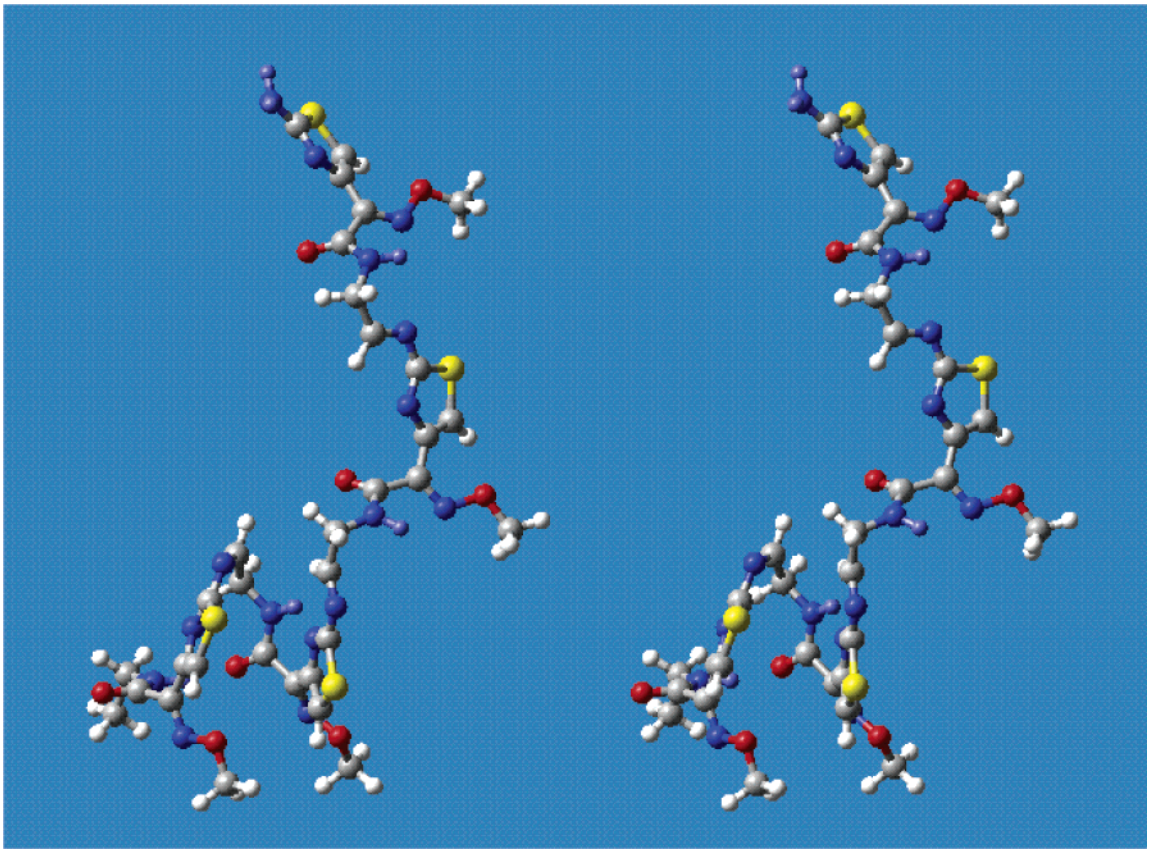

Figure 4. Stereoview of the lowest-energy tetramer conformer resulting from the MC conformational search.

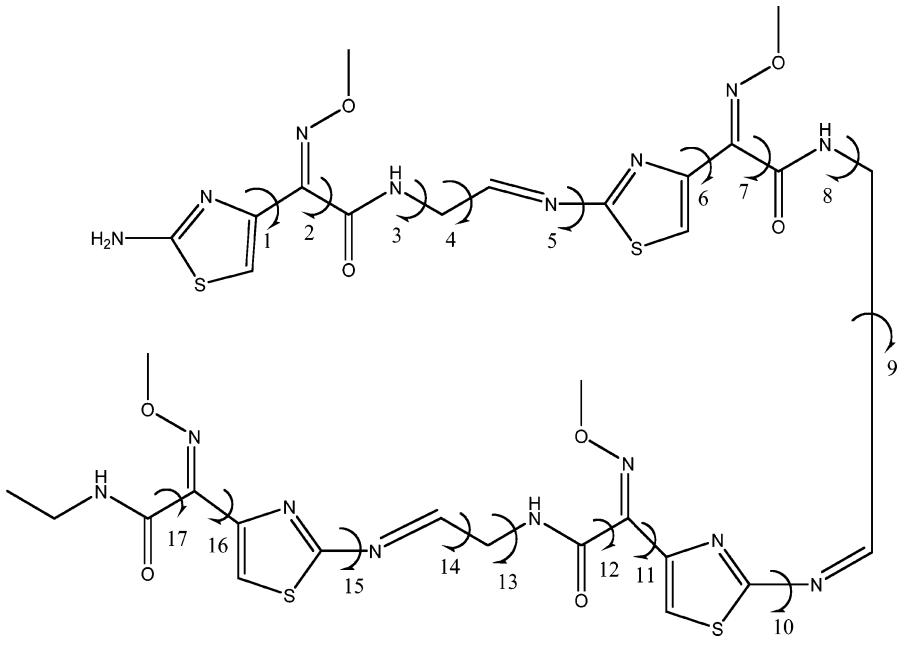

Figure 5. Numbering system for rotatable bonds in the tetramer.

conformer (Figure 6) remained essentially the same after minimization with implicit water (Table 1).

We built the hexamer by adding a monomer to the energy-minimized pentamer. Since all the new dihedral angles in the pentamer structure showed a large variation, we put constraints on the torsions according to the tetramer distribution analysis. Fifteen rotatable bonds (1, 4, 5, 7, 9, 18−27) were marked for exploration. Distribution analysis results from JMP revealed that most of the conformers had dihedral angle 18 near 87°, dihedral angle 19 near 74°, dihedral angle 20 near −48°, dihedral angle 21 near 157°, dihedral angle 22 near −85°, dihedral angle 24 near 84°, dihedral angle 25 near 4°, dihedral angle 26 near 143°, and dihedral angle 27 near 170° (Figure 7). The lowest-energy conformer is shown in Figure 8, and the results are tabulated in Table 1.

We built the octamer by adding a dimer to the energy-minimized hexamer reported above. We put constraints on the dihedral angles according to the hexamer distribution analysis mentioned in the above paragraph. Fifteen rotatable bonds were marked for exploration. The lowest-energy

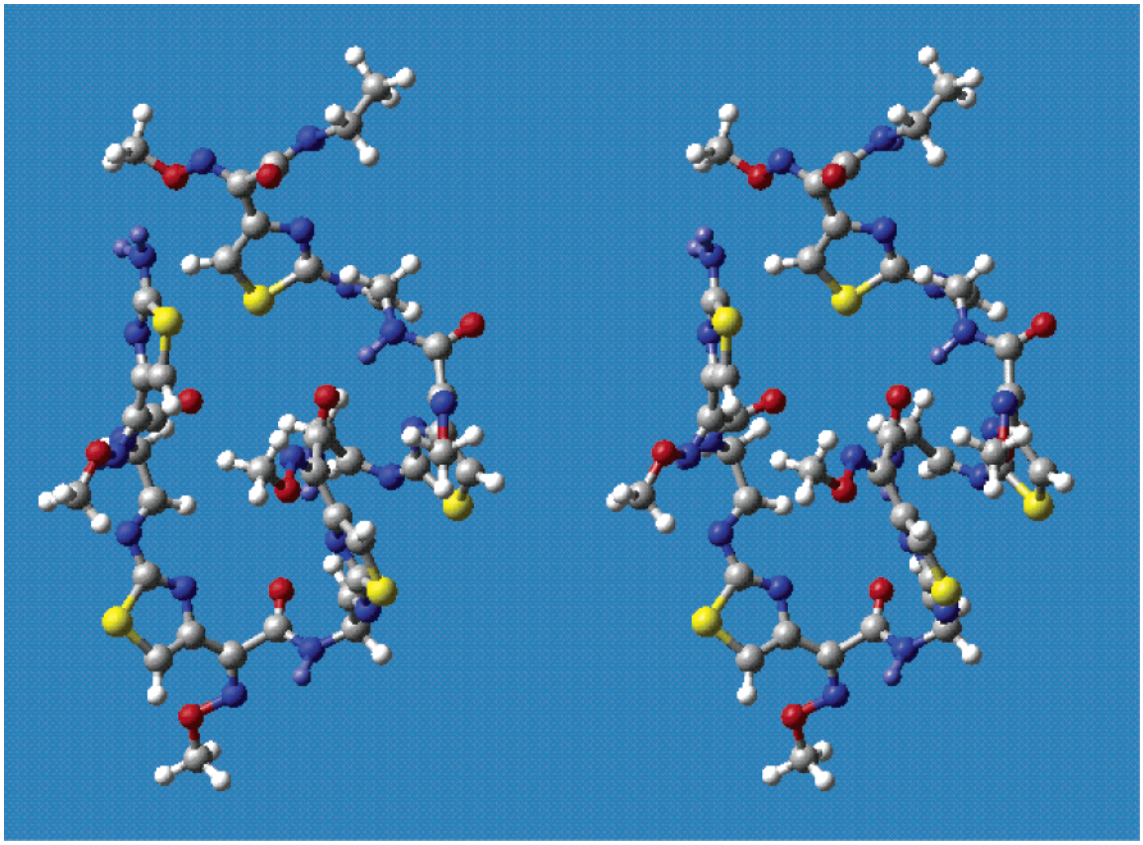

Figure 6. Stereoview of the lowest-energy pentamer conformer resulting from the MC conformational search.

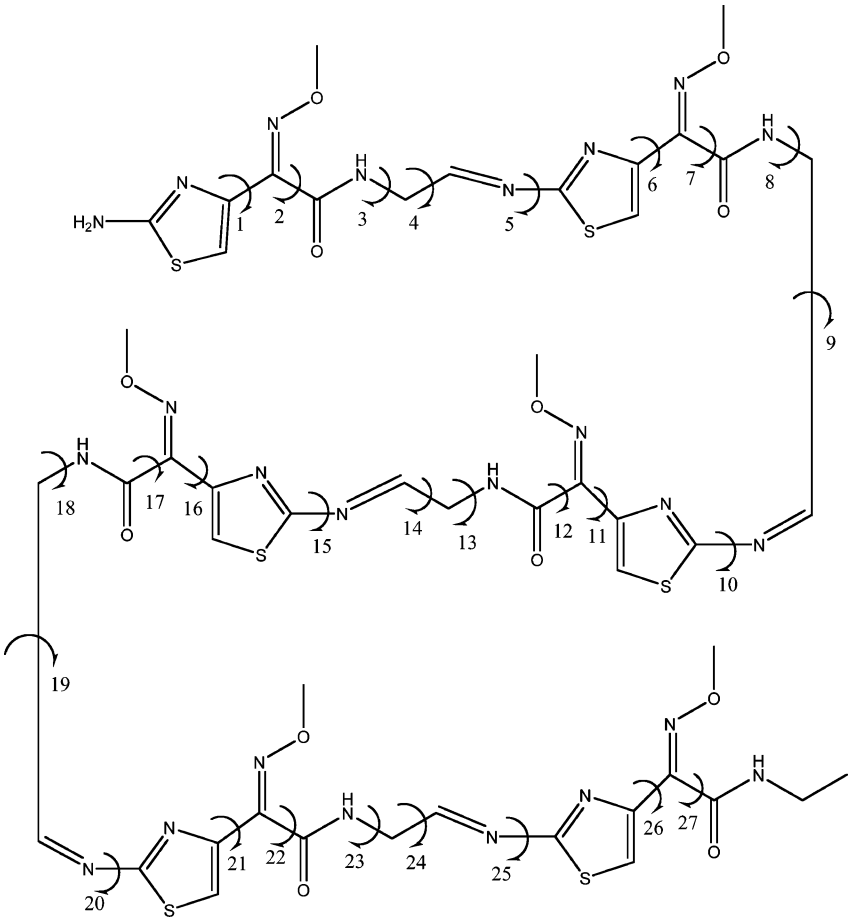

Figure 7. Numbering system for rotatable bonds in the hexamer.

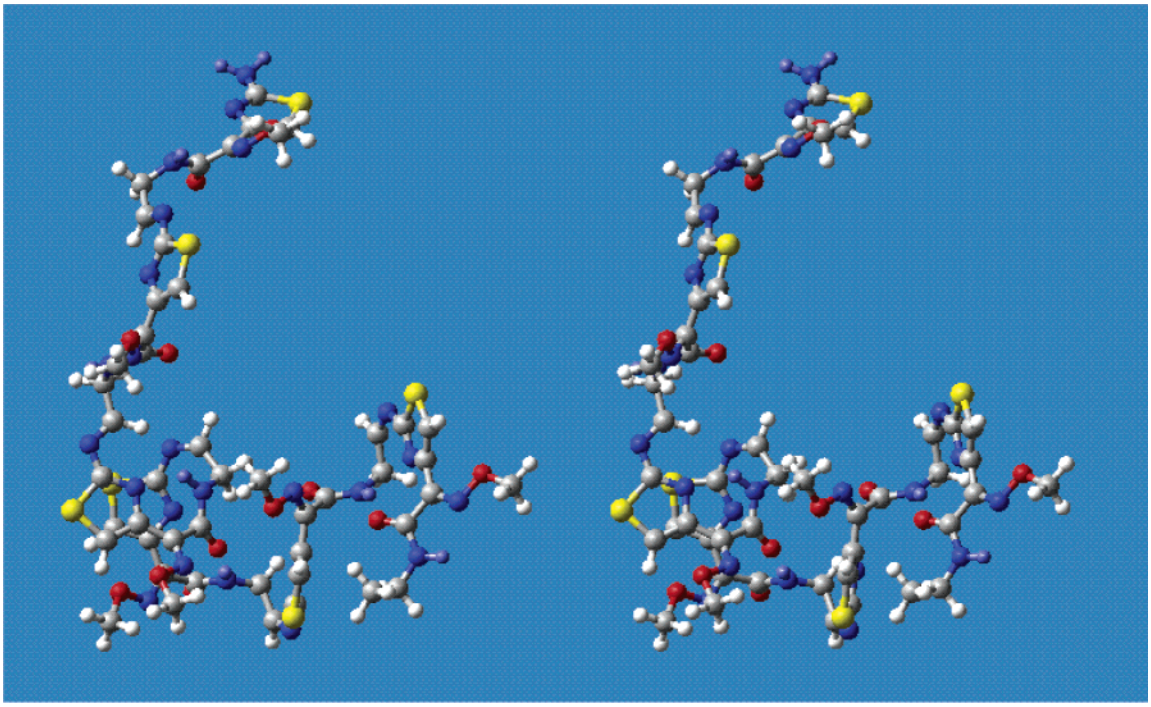

Figure 8. Stereoview of the lowest-energy hexamer conformer resulting from the MC conformational search.

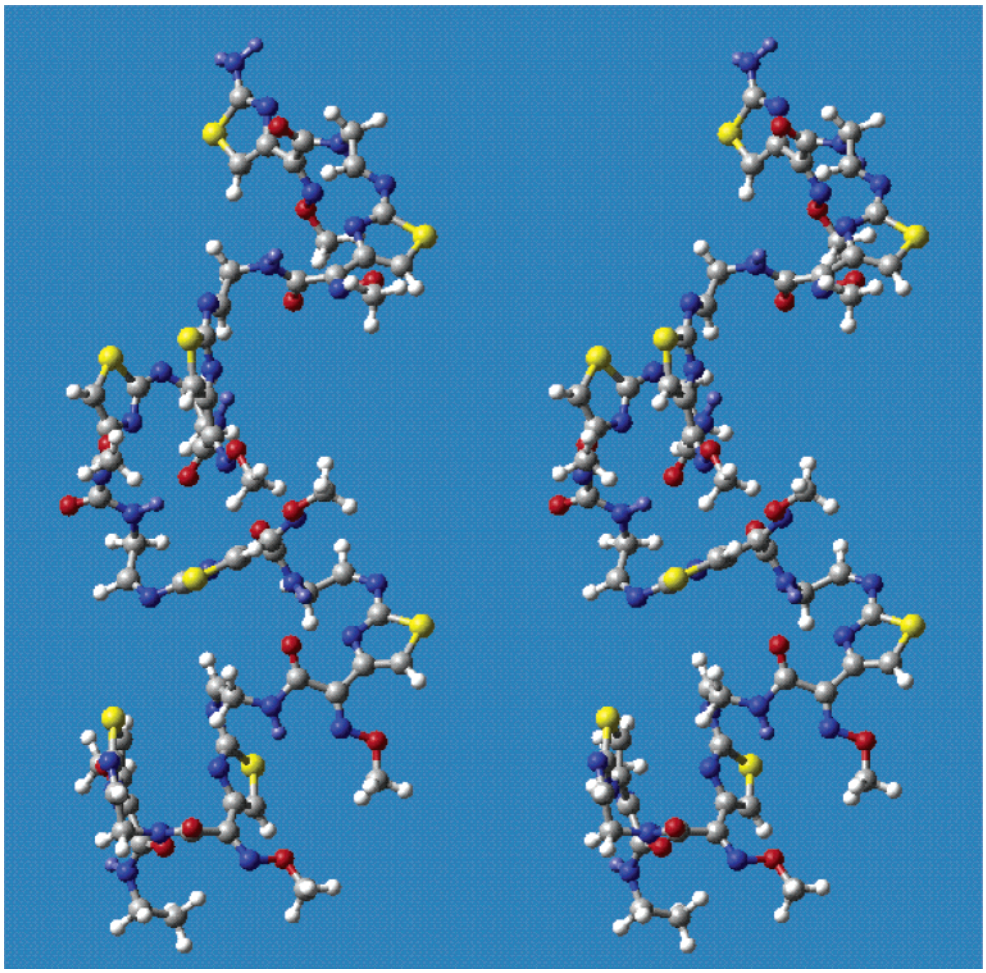

Figure 9. Stereoview of the lowest-energy octamer conformer resulting from the MC conformational search.

conformer (Figure 9) was minimized with implicit water as the solvent (Table 1).

At this point in our research, we had not observed any development of secondary structure or repetitive conformations in the growing polymer. We examined not only the lowest-energy conformers (as shown in the figures) but also other low-energy conformations. In some conformers, thiazole rings are positioned for stacking (see, e.g., Figure 9).

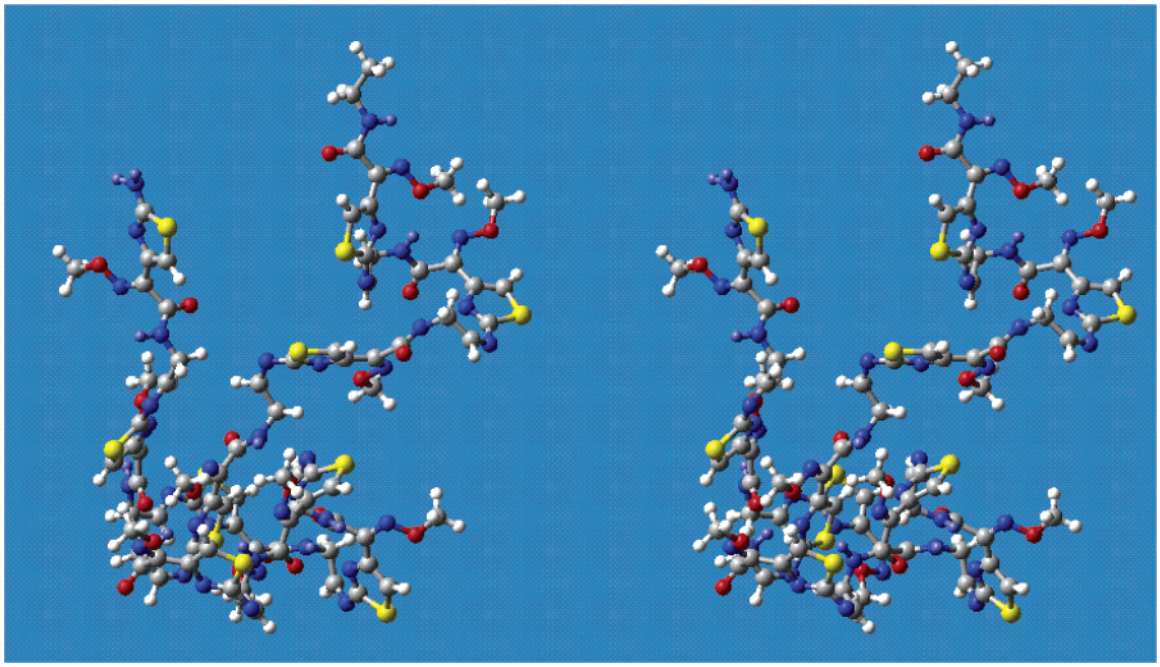

Figure 10. Stereoview of the lowest-energy decamer conformer resulting from the MC conformational search.

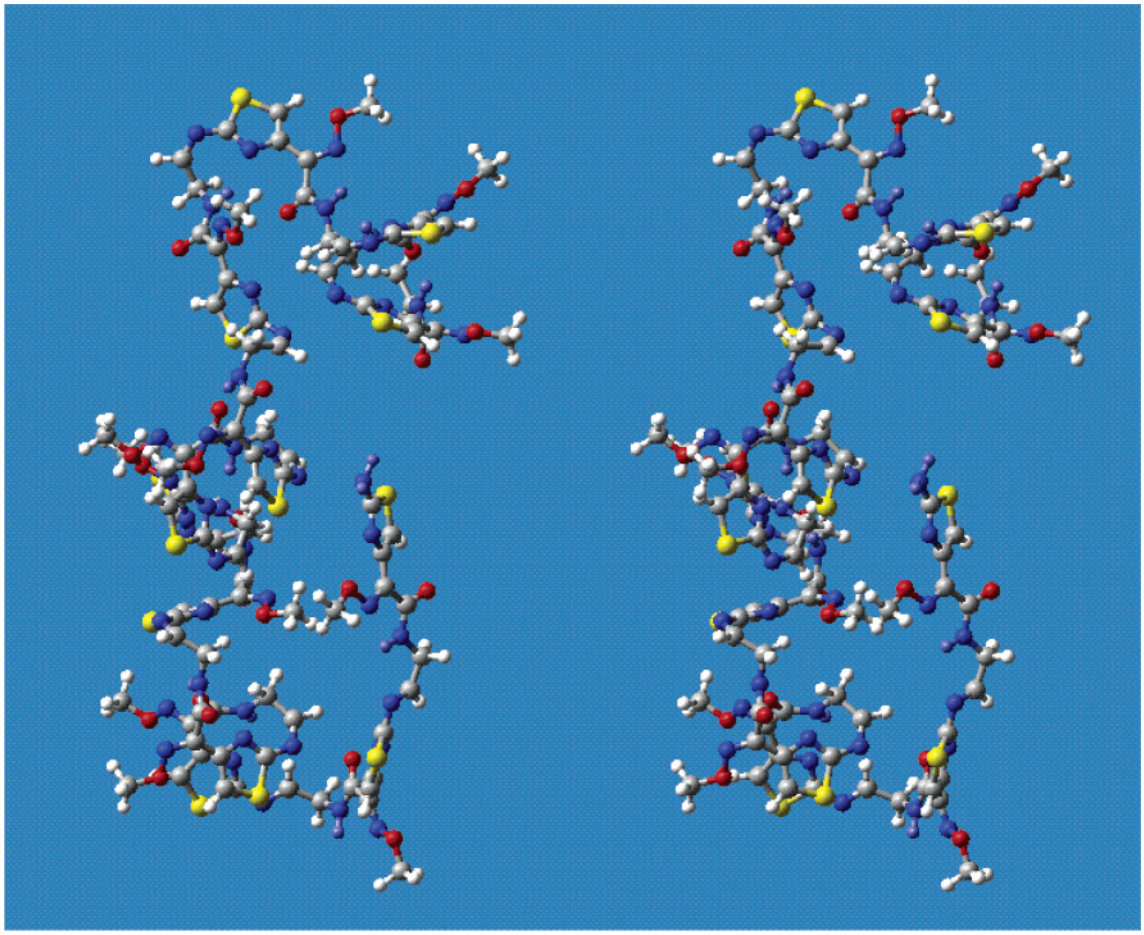

Figure 11. Stereoview of the lowest-energy 12-mer conformer resulting from the MC conformational search.

However, this arrangement does not appear to be predominant.

Because the final octamer structure was somewhat tangled (Figure 9), we experimented with starting the decamer in an extended conformation. We added a dimer to the energy-minimized octamer. The geometry of the decamer was energy-minimized with MMFF94 and a temporary distance constraint of 100 ± 10 Å between the nitrogen and carbon atoms at the two ends of the oligomer in order to stretch it out. This extended conformation was used directly as the starting geometry for the MC run. We did not put any constraints on the dihedrals in setting up the MC conforma-

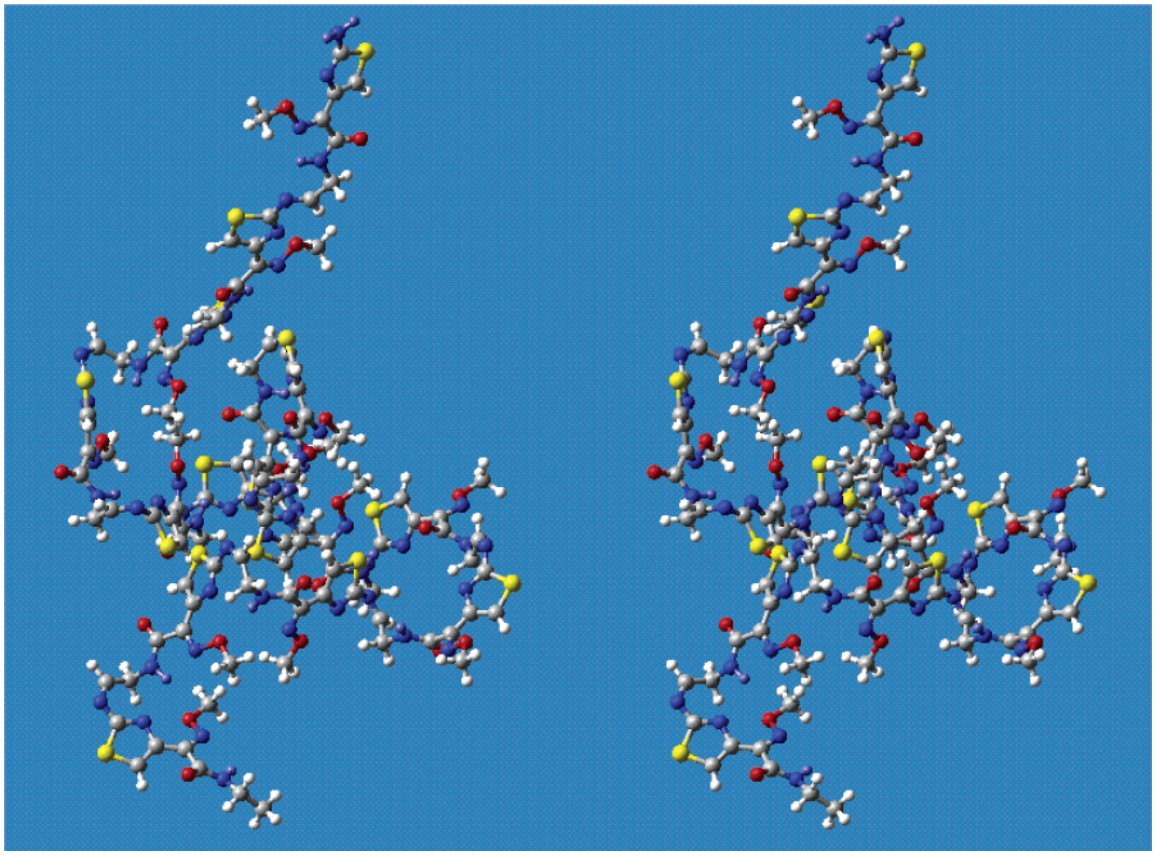

Figure 12. Stereoview of the lowest-energy 14-mer conformer resulting from the MC conformational search.

tional search of the 47 rotatable bonds, so there was no built-in preference for dihedral angle values found to be prevalent in the smaller oligomers. The MC run found 1659 allowed conformers, which is only about half as many as found for the hexamer (Table 1). The lowest-energy conformer is very compact (Figure 10).

The 12-mer was constructed by adding a dimer to the energy-minimized decamer. We minimized the 12-mer with a temporary distance constraint of 110 ± 10 Å between the terminal nonhydrogenic atoms in order to stretch out the oligomer to an extended starting conformation. We applied constraints to dihedral angles 10−17 of the three tetramer units (Figure 5) of the 12-mer according to the tetramer results. The MC search was run on 35 rotatable bonds. The lowest-energy conformer (Figure 11) had the energy shown in Table 1.

We built the 14-mer by adding a dimer to the energy-minimized 12-mer. We minimized the 14-mer with a temporary distance constraint of 120 ± 10 Å between the two ends of the molecule in order to stretch it to an extended conformation. We put no constraints on the MC conformational search of 67 rotatable bonds. The lowest-energy conformer (Figure 12) did not change its shape significantly when this structure was minimized with implicit water as the solvent. We see that the two termini project from a compact core consisting of 10 or 11 monomeric units.

Last, we built the 16-mer by adding a dimer to the energy-minimized 14-mer. We minimized the 16-mer with MMFF94 with a temporary distance constraint of 150 ± 10 Å between the terminal nonhydrogenic atoms in order to start with an extended conformation. We put no constraints on the MC conformational search of 77 rotatable bonds. The resulting number of allowed conformers is only 349 (Table 1) because the two "arms" emanating from each rotatable bond are sufficiently long and voluminous that they bump into other atoms frequently. The lowest-energy conformer is shown in Figure 13. To generate more conformers of the 16-mer, we tried minimizing the structure with MMFF94 with a little bit larger distance constraint of 155 ± 10 Å. Again, no constraints were put on the MC conformational search. The number of steps was increased to 650 000, and 77 rotatable bonds were again marked for exploration. When the MC run was complete, the number of allowed conformers had increased only marginally to 454 (Table 1). The lowest-energy conformer (Figure 14) was used as the starting structure for a third conformational search. The number of steps was set to 600 000, and no constraints were applied. This MC run generated a greater number of allowed conformers (Table 1). The lowest-energy conformer is shown in Figure 15. Again, the shape did not change significantly when the structure was energy-minimized in implicit water.

It can be seen in Figures 13−15 that the lowest-energy conformer from each of the three Monte Carlo runs of the 16-mer are quite different from each other. The shapes of the structures changed little during minimization. Note that the energies of the three minimized conformers (Table 1) are similar within 1 kcal/mol of each other. It is not surprising that a moderately flexible molecule like the ATMO polymer would exist in a population of diverse conformations, all with similar energy.

The declining efficiency of the MCMM method to generate allowable conformers as the molecular size of the oligomers increases is illustrated in Figure 16. Not surprisingly, it becomes much more difficult for the algorithm to find

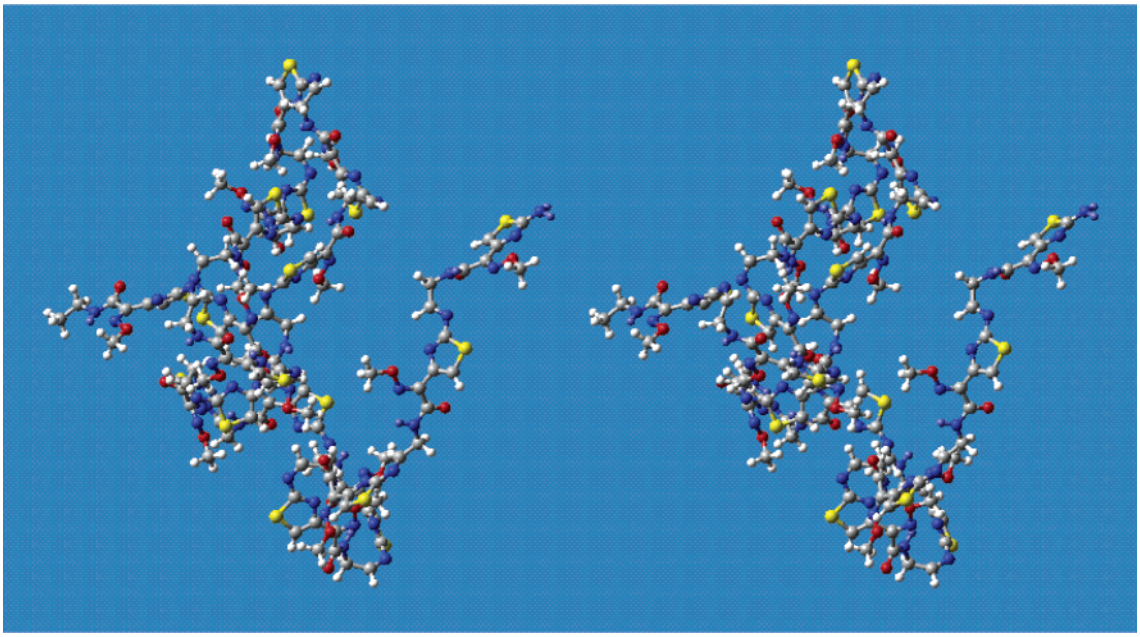

Figure 13. Stereoview of the lowest-energy conformer resulting from the first MC conformational search on the 16-mer.

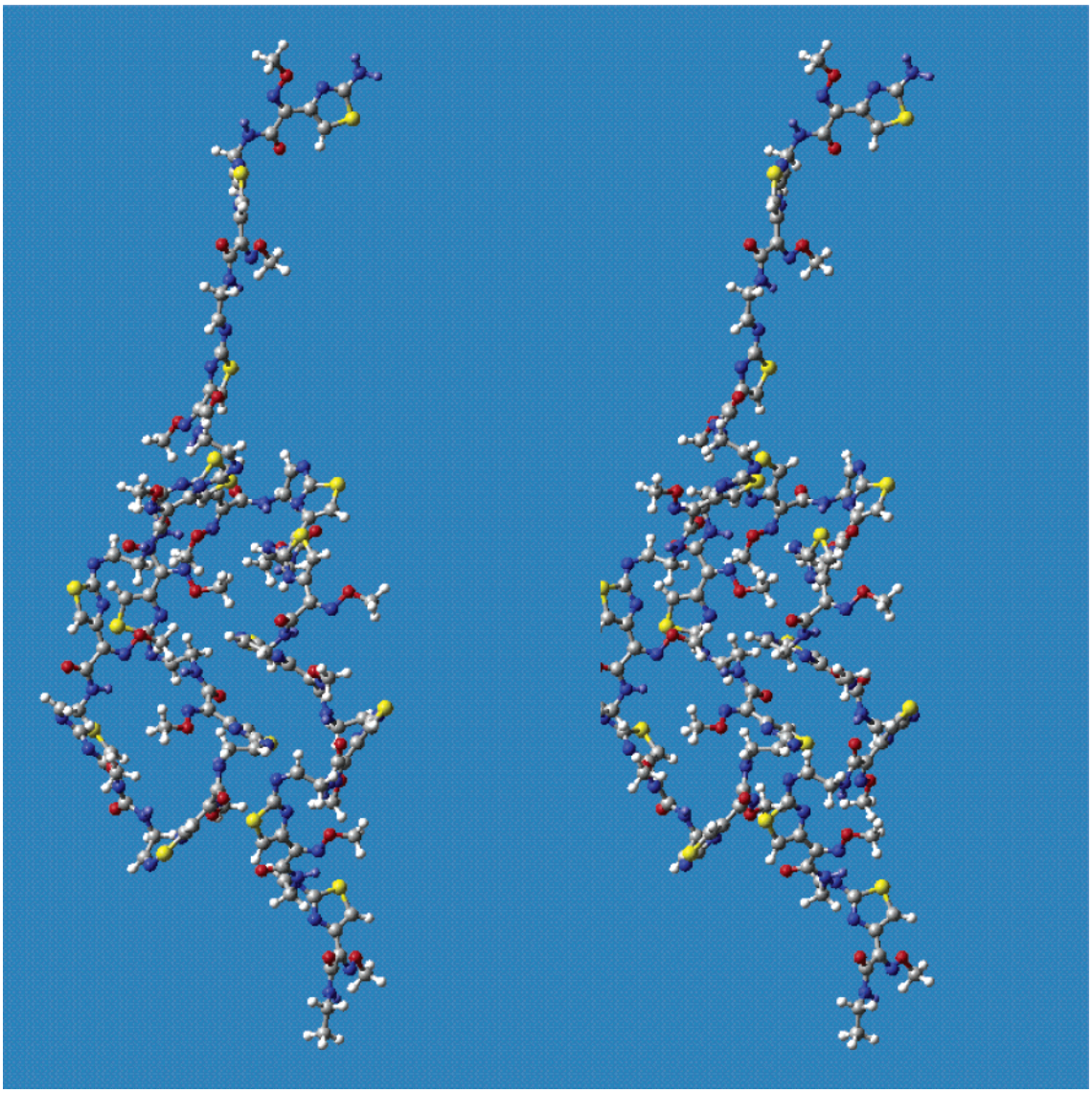

Figure 14. Stereoview of the lowest-energy conformer resulting from the second MC conformational search on the 16-mer.

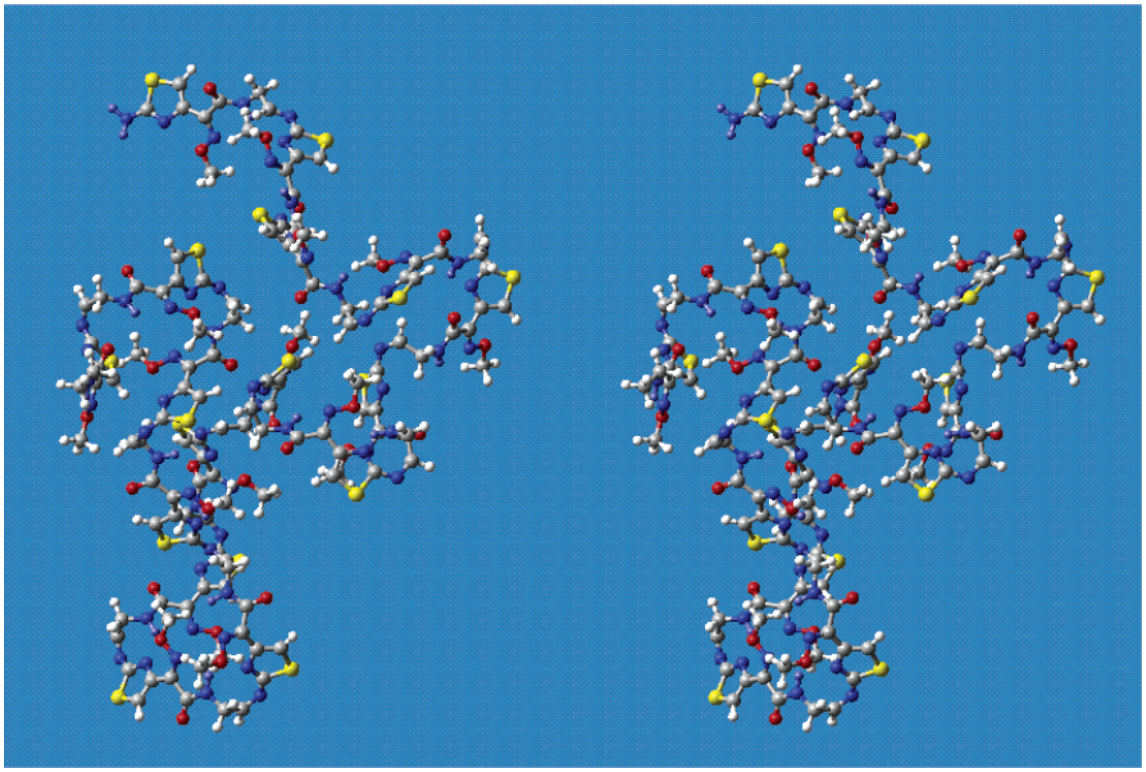

Figure 15. Stereoview of the lowest-energy conformer resulting from the third MC conformational search on the 16-mer.

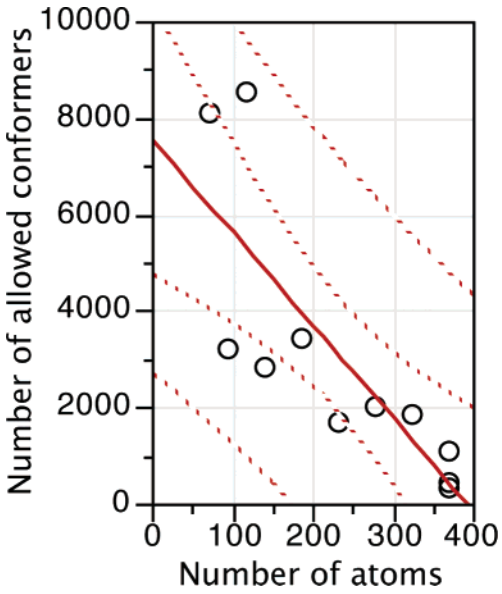

Figure 16. Relationship between the number of allowed conformers vs the number of atoms in the ATMO oligomers. Regression equation: number of allowed conformers = 7549.214 (±1225.419) − 19.201 (±4.728) number of atoms; $n = 11$; $r^2 = 0.647$; $r_{adj}^2 = 0.608$; RMS error = 1746.85; t ratios = 6.16, −4.06.

conformers that do not encounter steric clashes as the length of the molecule increases.

Molecular Similarity. We compared the chemical structures of the monomer and dimer forms of ATMO (Chart 1) with 28 other reported HIV-1 RT inhibitors.

The inhibitors represent a variety of compound classes.[2,5−9,39] Similarity was assessed using Daylight fingerprints in Tanimoto coefficient calculations.[37] As is well-known, fingerprints describe the connectivity in a molecule; they do not give a direct indication of the three-dimensional structure

Chart 1

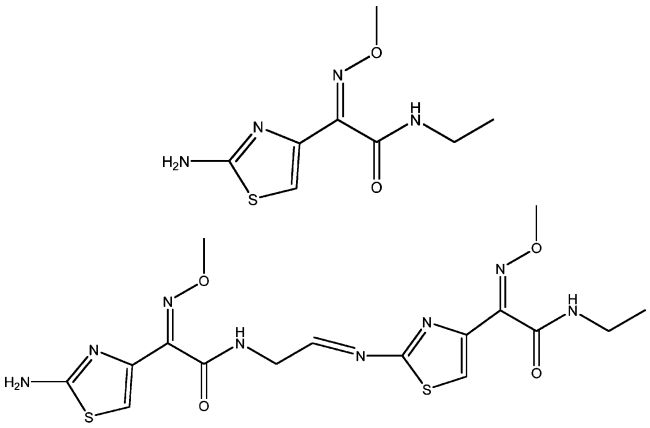

or of the presence of intra- or intermolecular interactions. The results show how unique the ATMO structure is compared to those of other known inhibitors. Similarity ratios are between 0.08 and 0.32, corresponding to very low similarity. The highest similarity (0.3245) is for a 1,3-thiazole-containing oligomer derivative (Chart 2) that inhibits HIV-1 integrase.[40] This finding is easily understandable because of the commonality of the thiazole ring and the amide linkages in the respective structures.

CONCLUDING REMARKS

The polymeric material formed from third-generation (ATMO-containing) cephalosporins offers an alternative, relatively unexplored approach to blocking the replication of HIV-1.

We determined the low-energy conformers of an ATMO polymer but, at least for the model we used, saw no evidence for the formation of secondary structure or repetitive

Chart 2

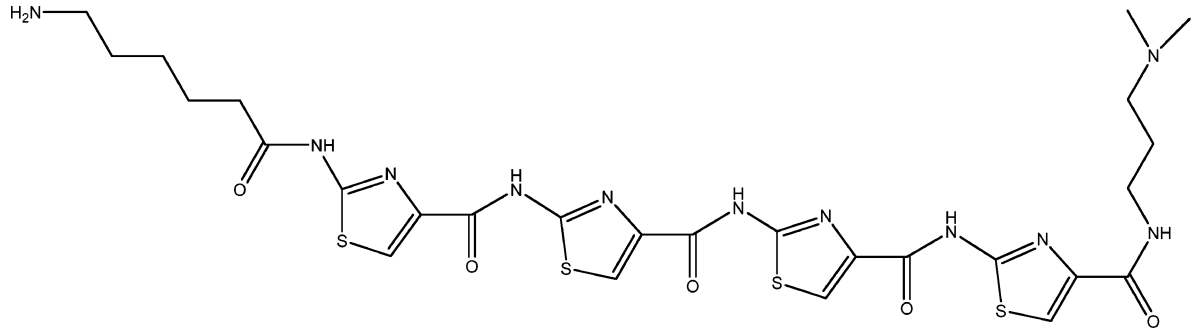

conformations in the growing polymer chain. Thus, until further computational and experimental studies are completed, one would have to regard the polymeric ATMO materials as existing predominantly in random coil conformations. Although one could conjecture that the ATMO polymer folds into a shape that resembles DNA, we saw no evidence for this in this preliminary study.

An interesting observation made by Hobi et al.[19] was that the high molecular weight polymer formed from ceftazidime (HMWP), besides inhibiting HIV-1 reverse transcriptase and RNase H activity, also appeared to act at a very early stage in the viral life cycle. The authors speculated that this early stage may be the process in which viral particles fuse to the victim cell membrane. As first discussed in the 1980s, certain sulfated polyanions inhibit HIV-1.[41,42] For instance, this inhibition is observed with sulfated polysaccharides with anticoagulant activity such as dextran sulfates (4−500 kDa), pentosan (xylan polysulfate, 1.5−5 kDa), and heparin (6−30 kDa). These polyelectrolytes not only block RNase H but may also interfere with virus uptake by the host cell. One could envision that HMWP formed from aged ceftazidime, because of its polyanionic nature, is similarly acting at two levels: blocking fusion and blocking RNase H. In contrast, polymers formed from third-generation cephalosporins without the carboxyl group in the 7-position side chain of ceftazidime could block reverse transcriptase but might be unable to interfere with fusion.

Although penicillins and cephalosporins are known primarily for their antibacterial properties, it is interesting to note that other biological activities have been detected. For instance, a degradation product from penicillin G (totally unrelated to the ATMO polymer) has inhibitory activity against HIV-1 protease.[43] Also, cephalosporins have been found to exhibit antimycotic activity.[44]

Ribonuclease H of human immunodeficiency virus requires Mn^{2+} or Mg^{2+}.[45−47] One possibility that could be explored in the future is to determine how well the ATMO polymer might chelate and sequester metal ions. In the molecular modeling done to date, we observed a few conformers of the oligomers that could present a coordination site for metal ions. Metal ions might change the conformation of the polymer and affect its binding to HIV-1 RT. These topics deserve further investigation. Docking experiments might also be of interest, but until the three-dimensional structures of the ATMO polymer are better understood, any docking alignment would be speculative.

ACKNOWLEDGMENT

We are grateful to Dr. Kelsey Forsythe for managing the hardware and software in our department and for consultation. We are also grateful to Dr. Steven Baertschi for his comments on the manuscript.

REFERENCES AND NOTES

(1) Romeo, D. L. Advances in the Development of HIV Reverse Transcriptase Inhibitors. *Annu. Rep. Med. Chem.* **1994**, *29*, 123−130.
(2) De Clercq, E. New Developments in Anti-HIV Chemotherapy. *Biochim. Biophys. Acta* **2002**, 258−275.
(3) Young, S. D. Recent Advances in the Chemotherapy of HIV. *Annu. Rep. Med. Chem.* **2003**, *38*, 173−181.
(4) De Clercq, E. New Approaches toward Anti-HIV Chemotherapy. *J. Med. Chem.* **2005**, *48*, 1297−1313.
(5) Min, B. S.; Nakamura N.; Miyashiro, H.; Kim, Y. H.; Hattori, M. Inhibition of Human Immunodeficiency Virus Type 1 Reverse Transcriptase and Ribonuclease H Activities by Constituents of Juglans mandshurica. *Chem. Pharm. Bull.* **2000**, *48*, 194−200.
(6) Min, B. S.; Miyashiro, H.; Hattori, M. Inhibitory Effects of Quinones on RNase H Activity Associated with HIV-1 Reverse Transcriptase. *Phytother. Res.* **2002**, *16*, S57−S62.
(7) Klarman, G. J.; Hawkins, M. E.; Le Grice, S. F. J. Uncovering the Complexities of Retroviral Ribonuclease H Reveals Its Potential as a Therapeutic Target. *AIDS Rev.* **2002**, *4*, 183−194.
(8) Andreola, M. L.; De Soultrait, V. R.; Fournier, M.; Parissi, V.; Desjobert, C.; Litvak, S. HIV-1 Integrase and RNase H Activities as Therapeutic Targets. *Expert Opin. Ther. Targets* **2002**, *6*, 433−446.
(9) Parniak, M. A.; Min, K. L.; Budihas, S. R.; Le Grice, S. F. J.; Beutler, J. A. A Fluorescence-Based High-Throughput Screening Assay for Inhibitors of Human Immunodeficiency Virus-1 Reverse Transcriptase-Associated Ribonuclease H Activity. *Anal. Biochem.* **2003**, *322*, 33−39.
(10) Shaw-Reid, C. A.; Munshi, V.; Graham, P.; Wolfe, A.; Witmer, M.; Danzeisen, R.; Olsen, D. B.; Carroll, S. S.; Embrey, M.; Wai, J. S.; Miller, Michael D.; Cole, J. L.; Hazuda, D. J. Inhibition of HIV-1 Ribonuclease H by a Novel Diketo Acid, 4-[5-(Benzoylamino)thien-2-yl]-2,4-dioxobutanoic Acid. *J. Biol. Chem.* **2003**, *278*, 2777−2780.
(11) De Clercq, E. Strategies in the Design of Antiviral Drugs. *Nat. Rev. Drug Discovery* **2002**, *1*, 13−25.
(12) Sevilya, Z.; Loya, S.; Hughes, S. H.; Hizi, A. The Ribonuclease H Activity of the Reverse Transcriptases of Human Immunodeficiency Viruses Type 1 and Type 2 Is Affected by the Thumb Subdomain of the Small Protein Subunits. *J. Mol. Biol.* **2001**, *311*, 957−971.
(13) Nanni, R. G.; Ding, J.; Jacobo-Molina, A.; Hughes, S. H.; Arnold, E. Review of HIV-1 Reverse Transcriptase Three-dimensional Structure: Implications for Drug Design. *Perspect. Drug Discovery Des.* **1993**, *1*, 129−150.
(14) Jager, J.; Smerdon, S. J.; Wang, J.; Boisvert, D. C.; Steitz, T. A. Comparison of Three Different Crystal Forms Shows HIV-1 Reverse Transcriptase Displays an Internal Swivel Motion. *Structure* **1994**, *2*, 869−876.
(15) Do, U. H.; Neftel, K. A.; Spadari, S.; Hübscher, U. Betalactam Antibiotics Interfere with Eukaryotic DNA-Replication by Inhibiting DNA Polymerase Alpha. *Nucleic Acids Res.* **1987**, *15*, 10495−10506. See also Neftel, K. A.; Hübscher, U. Effects of β-Lactam Antibiotics on Proliferating Eucaryotic Cells. *Antimicrob. Agents Chemother.* **1987**, *31*, 1657−1661. Neftel, K. A.; Hafkemeyer, P.; Cottagnoud, P.; Eich, G.; Hübscher, U. Did Evolutionary Forerunners of Betalactam-Antibiotics Bind to Nucleic Acid Replication Enzymes? In *50 Years of Penicillin Application-History and Trends*; Kleinkauf, H., von Dohren, H. Eds.; Public: Prague, 1993; pp 394−403.
(16) Hafkemeyer, P.; Neftel, K. A.; Hübscher, U. HIV−Reverse Transcriptase and Human DNA Polymerase Alpha Share Amino Acid Sequence Homologies to Bacterial Penicillin-Binding Proteins. *Methods Find. Exp. Clin. Pharmacol.* **1990**, *12*, 43−46.
(17) Hafkemeyer, P.; Neftel, K.; Hobi, R.; Pfaltz, A.; Lutz, H.; Luthi, K.; Focher, F.; Spadari, S.; Hubscher, U. HP 0.35, A Cephalosporin

Degradation Product Is a Specific Inhibitor of Lentiviral RNases H. *Nucleic Acids Res.* **1991**, *19*, 4059−4065.
(18) Baertschi, S. W.; Cantrell, A. S.; Kuhfeld, M. T.; Lorenz, L. J.; Boyd, D. B.; Jaskunas, S. R. Inhibition of Human Immunodeficiency Virus Type 1 Reverse Transcriptase by Degradation Products of Ceftazidime. *Antiviral Chem. Chemother.* **1997**, *8*, 353−362.
(19) Hobi, R.; Hübscher, U.; Neftel, K.; Alteri, E.; Poncioni, B.; Walker, M. R.; Woods-Cook, K.; Schneider, P.; Lazdins, J. K. Anti-HIV-1 Activity in vitro of Ceftazidime Degradation Products. *Antiviral Chem. Chemother.* **2001**, *12*, 109−118.
(20) Boyd, D. B. Unpublished data.
(21) Ercanli, T.; Boyd, D. B. Evaluation of Computational Chemistry Methods: Crystallographic and Cheminformatics Analysis of Aminothiazole Methoximes. *J. Chem. Inf. Model.* **2005**, *45*, 591−601.
(22) *Maestro*; Schrodinger Inc.: Portland, OR. http://www.schrodinger.com.
(23) Chang, G.; Guida, W. C.; Still, W. C. An Internal-Coordinate Monte Carlo Method for Searching Conformational Space. *J. Am. Chem. Soc.* **1989**, *111*, 4379−4386.
(24) Saunders, M.; Houk, K. N.; Wu, Y. D.; Still, W. C.; Lipton, M.; Chang, G.; Guida, W. C. Conformations of Cycloheptadecane. A Comparison of Methods for Conformational Searching. *J. Am. Chem. Soc.* **1990**, *112*, 1419−1427.
(25) Cramer, C. J.; Truhlar, D. G. Continuum Solvation Models: Classical and Quantum Mechanical Implementations. In *Reviews in Computational Chemistry*; Lipkowitz, K. B., Boyd, D. B., Eds.; VCH: New York, 1995; Vol. 6, pp 1−72.
(26) Reddy, M. R.; Erion, M. D.; Agarwal, A.; Viswanadhan, V. N.; McDonald, D. Q.; Still, W. C. Solvation Free Energies Calculated Using the GB/SA Model: Sensitivity of Results on Charge Sets, Protocols, and Force Fields. *J. Comput. Chem.* **1998**, *19*, 769−780.
(27) Gibson, K. D.; Scheraga, H. A. Revised Algorithms for the Build-Up Procedure for Predicting Protein Conformations by Energy Minimization. *J. Comput. Chem.* **1987**, *8*, 826−834.
(28) Scheraga, H. A. Predicting Three-Dimensional Structures of Oligopeptides. In *Reviews in Computational Chemistry*; Lipkowitz, K. B., Boyd, D. B., Eds.; VCH: New York, 1992; Vol. 2, pp 73−142.
(29) *JMP*, version 5.1; SAS Institute: Cary, NC. http://www.jmp.com.
(30) James, C. A.; Weininger, D.; Delany J. *Daylight Theory Manual*; Daylight Chemical Information Systems, Inc.: Mission Viejo, CA. http://www.daylight.com/dayhtml/doc/theory/theory.toc.html.
(31) Shemetulskis, N. E.; Weininger, D.; Blankley, C. J.; Yang, J. J.; Humblet, C. Stigmata: An Algorithm To Determine Structural Commonalities in Diverse Datasets. *J. Chem. Inf. Comput. Sci.* **1996**, *36*, 862−871.
(32) Guha, R.; Jurs, P. C. Using Similarity and Classification Methods to Determine Applicability of QSAR Models to Query Set Compounds. Abstracts of Papers, 228th American Chemical Society National Meeting, Philadelphia, PA, August 22−26, 2004; COMP 191.
(33) Guha, R. *CDK Web Services: Similarity Calculator*; The Pennsylvania State University: State College, PA, 2005. http://blue.chem.psu.edu/~rajarshi/code/java/cdkws.html.
(34) Weininger, D. SMILES, A Chemical Language and Information System. 1. Introduction to Methodology and Encoding Rules. *J. Chem. Inf. Comput. Sci.* **1988**, *28*, 31−36.
(35) *ChemDraw Ultra*, version 8.0; Cambridgesoft Corp.: Cambridge, MA, 2005. http://products.cambridgesoft.com/family.cfm?FID=2.
(36) Helson, H. A. Structure Diagram Generation. In *Reviews in Computational Chemistry*; Lipkowitz, K. B., Boyd, D. B., Eds.; Wiley-VCH: New York, 1999; Vol. 13, pp 313−398.
(37) Leach A. R. *Molecular Modelling Principles and Applications*, 2nd ed.; Pearson: Essex, U. K., 2001; pp 676−677.
(38) Jorgensen, W. L.; Gao, J. Cis−Trans Energy Difference for the Peptide Bond in the Gas Phase and in Aqueous Solution. *J. Am. Chem. Soc.* **1988**, *110*, 4212−4216.
(39) Ercanli, T. M.S. Thesis, Indiana University−Purdue University−Indianapolis, Indianapolis, Indiana, 2005.
(40) Ryabinin, V. A.; Sinyakov, A. N.; de Soultrait, V. R.; Caumont, A.; Parissi, V.; Zakharova, O. D.; Vasyutina, E. L.; Yurchenko, E.; Bayandin, R.; Litvak, S.; Tarrago-Litvak, L.; Nevinsky, G. A. Inhibition of HIV-1 Integrase-Catalysed Reaction by New DNA Minor Groove Ligands: The Oligo-1,3-Thiazolecarboxamide Derivatives. *Eur. J. Med. Chem.* **2000**, *35*, 989−1000.
(41) Cowan, J. A.; Ohyama, T.; Howard, K.; Rausch, J. W.; Cowan, S. M. L.; Le Grice, S. F. J. Metal-Ion Stoichiometry of the HIV-1 RT Ribonuclease H Domain: Evidence for Two Mutually Exclusive Sites Leads to New Mechanistic Insights on Metal-Mediated Hydrolysis in Nucleic Acid Biochemistry. *J. Biol. Inorg. Chem.* **2000**, *5*, 67−74.
(42) Moelling, K.; Schulze, T.; Diringer, H. Inhibition of Human Immunodeficiency Virus Type 1 RNase H by Sulfated Polyanions. *J. Virol.* **1989**, *63*, 5489−5491.
(43) Humber, D. C.; Cammack, N.; Coates, J. A. V.; Cobley, K. N.; Orr, D. C.; Storer, R.; Weingarten, G. G.; Weir, M. P. Penicillin Derived C_2−Symmetric Dimers as Novel Inhibitors of HIV-1 Proteinase. *J. Med. Chem.* **1992**, *35*, 3080−3081.
(44) Sanyal, A. K.; Chowdhury, B.; Banerjee, A. B. Generation of High Antimycotic Activity During Degradation of β-Lactam Antibiotics. *Lett. Appl. Microbiol.* **1992**, *14*, 221−223.
(45) Starnes, M. C.; Cheng, Y.-C. Human Immodeficiency Virus Reverse Transcriptase-associated RNase H Activity. *J. Biol. Chem.* **1989**, *264*, 7073−7077.
(46) Davies, J. F., II; Hostomska, Z.; Hostomsky, Z.; Jordan, S. R.; Matthews, D. A. Crystal Structure of the Ribonuclease H Domain of HIV-1 Reverse Transcriptase. *Science* **1991**, *252*, 88−95.
(47) De Clercq, E. Antiviral Agents: Characteristic Activity Spectrum Depending on the Molecular Target With Which They Interact. *Adv. Virus Res.* **1993**, *42*, 1−55.

CI050339A